### Title
Temporal variation of intermediate-depth earthquakes around the time of the M9.0 Tohoku-oki earthquake




### Journal
Geophysical Research Letters, 44(8)

### ISSN
0094-8276



### Authors
Delbridge, Brent G
Kita, Saeko
Uchida, Naoki
et al.



### Publication Date
2017-04-28

### DOI
10.1002/2017gl072876

Peer reviewed

# Temporal variation of intermediate-depth earthquakes around the time of the *M*9.0 Tohoku-oki earthquake

Brent G. Delbridge

Saeko Kita

Naoki Uchida

Christopher W. Johnson

Toru Matsuzawa
Roland Bürgmann
First published: 05 April 2017

**https://doi.org/10.1002/2017GL072876**
**UC-eLinks**


## Abstract

The temporal evolution of intermediate-depth seismicity before and after the 2011 *M*9.0 Tohoku-oki earthquake reveals interactions between plate interface slip and deformation in the subducting slab. We investigate seismicity rate changes in the upper and lower planes of the double seismic zone beneath northeast Japan using both a $\beta$ statistic approach and a temporal epidemic type aftershock sequence model. We do not observe an anomalous precursory increase in intermediate-depth earthquake activity preceding the mainshock; however, following the mainshock, we observe a rate increase for the intermediate-depth earthquakes in the upper plane. The average ratio of upper plane to lower plane activity and the mean deep aseismic slip rate both increased by factor of 2. An increase of downdip compression in the slab resulting from coseismic and postseismic deformation enhanced seismicity in the upper plane, which is dominated by events accommodating downdip shortening from plate unbending.

# 1 Introduction

The locked zone between subducting and overriding plates hosts the largest earthquakes, including all the recorded events of moment magnitude (*M*) 9.0 or larger. However, a large

percentage of subduction zone earthquakes are intraslab events that occur within the subducting plate rather than along the plate boundary. These earthquakes are often damaging events that pose a seismic hazard to large populations along convergent boundaries across the globe. In general, we have a limited understanding of the physical mechanisms controlling the generation and occurrence of these events due to a lack of direct observation of composition, in situ stress state and insufficient understanding of their spatiotemporal distribution.

Previous studies have proposed models for the mechanisms controlling the large-scale stress regimes generated during the subduction process and the relation between intermediate-depth earthquakes and events on the plate boundary subduction thrust [*Dmowska et al*., 1988; *Thatcher and Rundle*, 1984; *Lay et al*., 1989]. In these models stresses are generated by the episodic locking of the upper part of the plate that only slides during large megathrust events. As the slab subducts into the surrounding mantle, a static stress field is generated by bending and unbending, slab-pull, and viscous resistance. The time varying stresses are superimposed on the static stress fields resulting in a temporally pulsating stress field. A mechanical model of the coupled subduction zone is presented by *Dmowska et al.* [1988], which argues for increased rates of intermediate-depth events indicating downdip extension prior to large interplate thrust events on timescales of months to years. This increase in the occurrence of extensional intraplate earthquakes in the subducting slab reflects the long-term stress cycle of the megathrust. On much shorter time scales (minutes to months) similar models suggest that transient slip downdip from the megathrust rupture zone results in diminished tensional stresses within the subducting slab [e.g., *Thatcher and Rundle*, 1984; *Dmowska et al.*, 1988], and furthermore, this slip could act as a precursor to the main rupture [*Obara and Kato*, 2016]. Thus, we expect an overall increase in the downdip tensional stress during the interseismic period, which is released over short timescales prior to, during and following the mainshock. *Lay et al.* [1989] examined global seismicity for temporal variations of intraplate seismic activity in the vicinity of large interplate thrust events. They show that the intermediate-depth seismicity rates exhibit strong spatiotemporal variations following large interplate thrust events and a transition from downdip tension to downdip compression caused by several great subduction thrust earthquakes.

Beneath the northeastern Japan arc (Tohoku region), intraslab earthquakes occur at depths of 50–200 km within the subducting slab. These events form two inclined parallel planes of seismicity separated by ~35 km which delineate the plate curvature as it subducts into the surrounding mantle. At depths >70 km beneath NE Japan the earthquake focal mechanisms of the upper plane predominantly reflect downdip compression, while the lower plane events reflect downdip extension [*Hasegawa et al.*, 1978; *Igarashi et al*., 2002]. Using 2002–2007 focal mechanism data

from the Kiban observation network, *Kita et al.* [2010a, 2010b] relocated the hypocenters at depths of 20–300 km beneath NE Japan and defined the location of a stress neutral plane between the double-layered seismic zone. A schematic interpretation is shown in Figure 1c of the relocations and the stress inversion results from *Kita et al.* [2010a, 2010b].

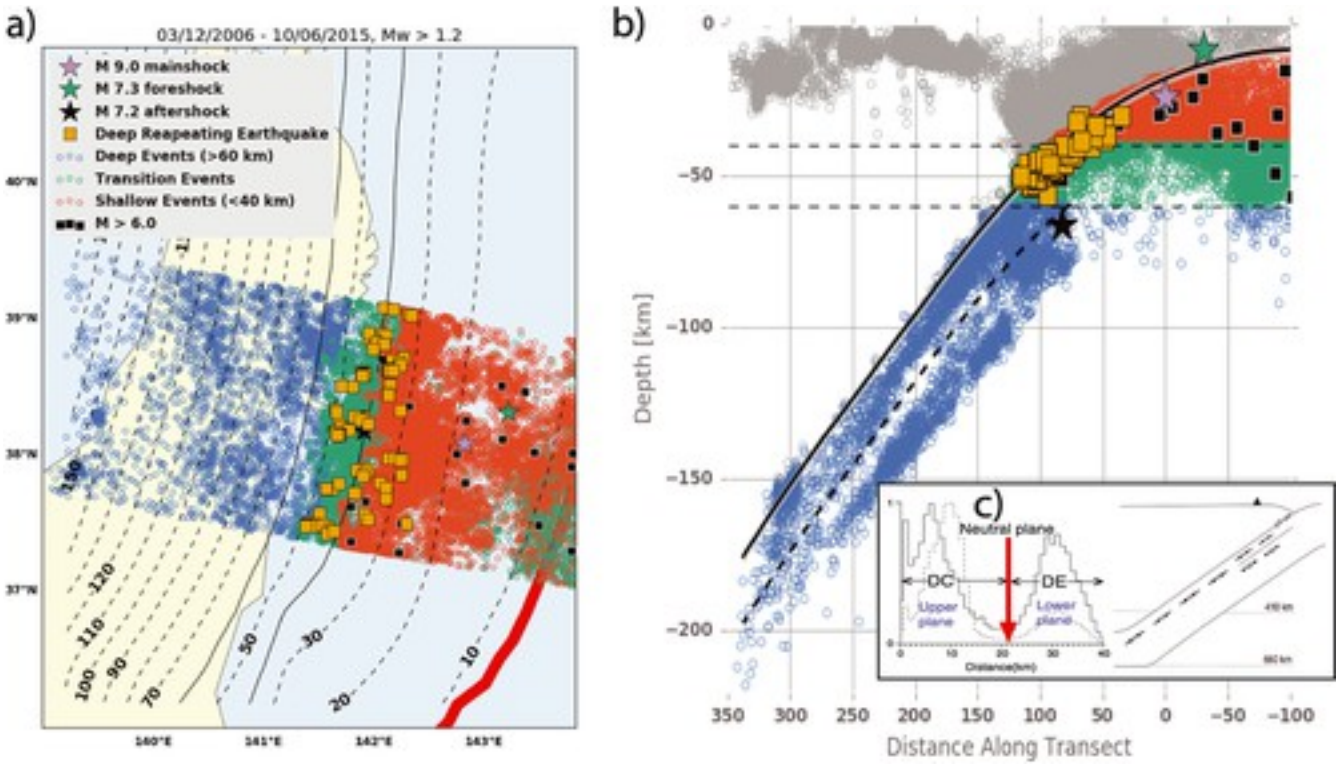


**Figure 1**

**Open in figure viewerPowerPoint**

JMA hypocenters selected for analysis (a) in map view and (b) in cross section. Shallow events are defined to have depths less than 40 km (red), and deep events are defined to have depths greater than 60 km (blue). Green and grey circles are events located in the transition depth range (40–70 km) and overriding plate, respectively, which were not included in the analysis. The purple, green, and black stars denote the locations of the 11 March 2011 *M*9.0 mainshock, 9 March 2011 *M*7.3 foreshock, and 7 April 2011 *M*7.2 aftershock. The black squares denote $M > 6.0$ earthquakes. The orange squares represent the repeating earthquakes used to estimate the deep aseismic slip rate in Figure 3b. The plate interface depth contours are shown by dashed and continuous black lines in Figure 1a [*Zhao et al.*, 1997; *Kita et al.*, 2010a, 2010b]. The solid and dashed black lines in Figure 1b are a smoothed representation of the plate interface within the transect and the location of the neutral plane at 22 km plate-interface depth. (c) Schematic interpretation of stress inversion results for NE Japan from *Kita et al.* [2010a, 2010b] with the normalized event frequency, including and excluding the aftershocks of the 2003 Miyagi-oki intraplate earthquake. The red arrow denotes the location of the inverted neutral plane. Gray and open dots in the right panel show downdip compression and downdip tension, respectively.

A recent seismicity analysis by *Bouchon et al.* [2016] suggests that the stress field associated with slab-pull should not be considered a static background stress but instead can vary temporally and directly or indirectly modulate both intermediate-depth and shallow earthquake activity. They analyze the intermediate-depth earthquake activity prior to the 11 March 2011 *M*9.0 Tohoku-oki earthquake and suggest that a 2 month long period of accelerated seismicity within the subducting slab occurred synchronously with shallow foreshock activity near the Tohoku-oki earthquake hypocenter. *Kato et al.* [2012] used foreshocks and small repeating earthquakes to show that an increase in shallow seismicity was driven by slow slip near the mainshock rupture area. Ocean bottom pressure gauge data also support this idea [*Ito et al*., 2013]. *Bouchon et al.* [2016] propose that the slab was transiently "stretching" and "plunging" below the rupture area of the Tohoku-oki earthquake and that this mechanism may more generally act as a nucleation phase for large megathrust earthquakes. The key difference between this new model and the previous studies is the source of the time-varying stress field. *Bouchon et al.* [2016] suggest that the temporal variation comes from transient deformation (over short timescales) within the slab, which increases the tensional stresses within the plate downdip of the megathrust and promotes slip on the shallow plate interface. This is in contrast to the alternative view [e.g., *Dmowska et al*., 1988] that slip may initiate along the downdip portion of the locked interface, which would result in increased downdip compression within the subducting plate.

In this study we examine the spatiotemporal variation of the intermediate-depth earthquake activity in the Tohoku region prior to and following the *M*9.0 rupture. We expect the increase in downdip compressional stress associated with the *M*9.0 mainshock (10–100 kPa [*Hu et al*., 2016]) to increase seismic activity in the downdip compressional upper plane and suppress activity in the downdip extensional lower plane. We examine seismicity rates in the layers to test whether the observations indicate an increase or decrease in the downdip tensional stresses, before and after the Tohoku-oki earthquake.

# 2 Data and Methods

## 2.1 JMA Hypocenters and Slab Geometry

To examine the temporal changes of seismicity within the subducting Pacific Plate, we analyze earthquake hypocenters from the Japan Meteorological Agency (JMA) catalog. The JMA catalog utilizes the Kiban Observation Network that was completed in 2002 and now includes more than 1200 stations and records ~100,000 events per year in Japan. The magnitude of completeness ($M_c$) in the Pacific slab beneath northeastern Japan is *M*1.2 [*Kita*, 2009] and increases to *M*3.0

near the trench [*Nanjo et al*., 2010]. We determine $M_c$ before and after the *M*9.0 mainshock for the deep intermediate-depth earthquakes (60–300 km) located within the transect shown in Figure 1 using goodness-of-fit (GFT) [*Wiemer and Wyss*, 2000] and maximum curvature (MAXC) [*Wiemer and Katsumata*, 1999]. Prior to the mainshock, we find a magnitude of completeness of *M* 1.4 ± 0.3 from GFT and *M*1.15 from MAXC (Figures S1a–S1c in the supporting information). Following the mainshock we find that the magnitude of completeness increased to *M*1.90 ± 0.3 for GFT and M2.17 from MAXC (Figures S1d–S1f). Figure S2 shows the magnitude of completeness versus time. With the exception of a brief excursion in March 2007 and directly following the *M*9.0 mainshock, the temporal $M_c$ estimates fall within the pre-mainshock and post-mainshock estimates (Figure S3). During the period directly following the mainshock, we also observe a sudden increase in the minimum measured magnitude (Figure S4); both the increased magnitude of completeness and minimum measured magnitude return to the post-mainshock average values within 6 months.

In the Tohoku region, interplate thrust events are limited to depths <60 km [*Igarashi et al*., 2003; *Kita et al*., 2010b]. The events used in this analysis are shown in map view and cross section in Figure 1 for a 200 km wide transect centered on the epicenter of the 2011 *M* 9.0 Tohoku-oki mainshock and approximately parallel with the slab dip (azimuth 275°). In order to determine the spatial distribution of earthquakes within the slab, we utilize a high-resolution slab geometry model of the plate interface. The shallow portion of the plate interface (<60 km depth) is determined from the location of low-angle thrust-fault events and repeating earthquakes [*Igarashi et al*., 2003; *Uchida et al*., 2003, 2009] and the deeper interface is resolved in large part from converted SP seismic waves [*Zhao et al*., 1997] and hypocenters [*Kita et al*., 2010a]. We omit earthquakes located within the overriding continental wedge and limit our analysis to the subducting slab using the plate-interface geometry (Figure 1). We calculate the minimum perpendicular distance of each hypocenter to the slab interface and select events within the slab using this distance, which we refer to as the plate-interface depth [*Zhao et al*., 1997; *Kita et al*., 2010a, 2010b]. The geometric selection process results in 7883 intermediate-depth (60–220 km) events and 22,392 shallow (0–60 km) events with magnitude greater than *M*1.2 from March 2006 to October 2015. We further separate the intermediate-depth region into two distinct planes of seismicity based on the location of the neutral plane (plate-interface depth of 22 km as shown by dashed line in Figure 1b) defined by *Kita et al*. [2010a, 2010b]. We select 5257 events in the compressional upper plane with a plate-interface depth < 22 km and 2626 events in the extensional lower plane with a plate-interface depth > 22 km.

## 2.2 Seismicity Rates

The seismicity is analyzed using three methods to determine temporal rate variations. First, we examine the earthquake activity spanning the time of the *M*9.0 mainshock by estimating the earthquake occurrence rate as a function of time using a 30 day bin width with a 12 h step for a lower magnitude cutoff of $M \geq 1.5$ to $M \geq 3.0$ with a 0.5 magnitude step for all cataloged events in the target volume (Figure 2a). All moving averages calculated in this study use an adaptive moving window to avoid averaging across a discrete change point ($t_c$), to avoid mixing preshock and postshock behavior [*Pollitz et al*., 2012; *Johnson et al*., 2015]. Earthquake occurrence rates are estimated at discrete times ($t_i$) with a moving window half width of $T_{hw}$ (here 15 days). For all times before the change point ($t_i < t_c$), the moving average bins are defined as $[t_i - T_{hw}, \min(t_c, t_i + T_{hw})]$ and for times after the change point ($t_i > t_c$) the bins are defined as $[\max(t_i - T_{hw}, t_c), t_i + T_{hw}]$. Additionally, we compare the cumulative number of events during the time of interest to the linear background rate estimated using both 1 and 5 years prior to the time of the *M*9.0 mainshock (supporting informationFigure S1).

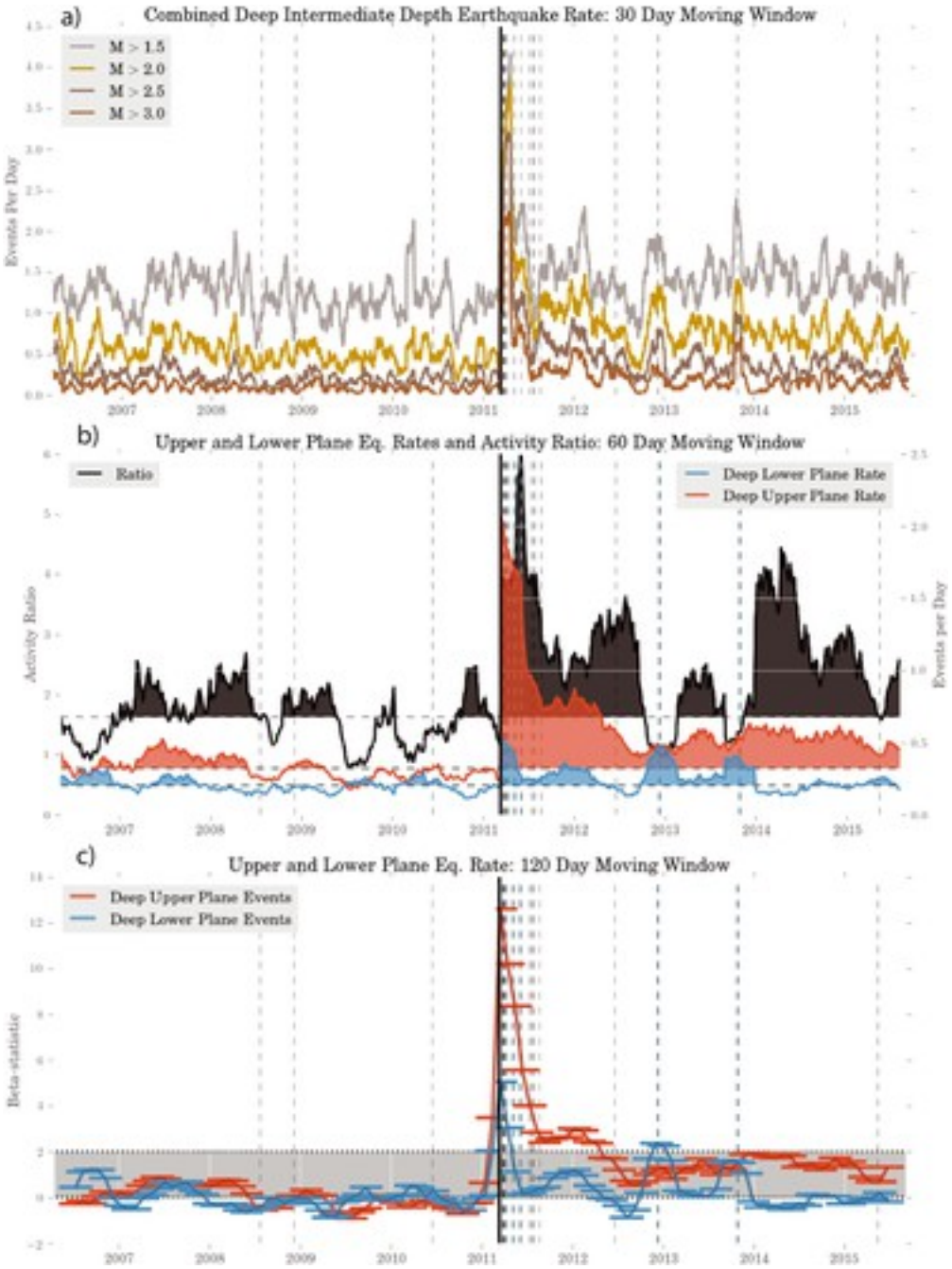


**Figure 2**

**Open in figure viewerPowerPoint**

Intermediate-depth (60–220 km) intraplate earthquake rate before and after the *M*9.0 Tohoku-oki mainshock from March 2006 to October 2015. (a) Intermediate-depth intraplate occurrence rate for a range of minimum magnitudes. The earthquake occurrence rate is calculated using a 30 day moving window and 2 day time steps. (b) Earthquake occurrence rate versus time separated into events in the upper (red) and lower (blue) seismicity planes. The black curve shows the ratio of the rates of upper over lower plane events. The filled regions under the curve denote periods exceeding the preforeshock average rate shown by the horizontal dashed black line. (c) $\beta$ statistic through time using the geometry shown in Figure 1 and a minimum cutoff of *M*2.0. The red and

blue curves represent the results for the upper plane events and lower plane events, respectively. The $\beta$ statistic is calculated using a 120 day moving window and 30 day time steps. The vertical black dashed lines show the origin times of large magnitude earthquakes ($M$ > 6.0) within the transect. The vertical blue dashed lines show the origin times of large magnitude earthquakes ($M$ > 6.0) within the lower plane. The solid black line shows the time of the $M$9.0 11 March Tohoku-oki mainshock. The horizontal grey region denotes the range of rate change from $\beta$ = 0 (no deviation from background rate), to $\beta$ = 2 (a statistically significant deviation).

Second, we investigate seismicity changes using the $\beta$ statistic approach [e.g., *Hough*, 2005; *Matthews and Reasenberg*, 1988; *Reasenberg and Simpson*, 1992]. Beta is defined as $\beta = \frac{N_a - N_e}{\sqrt{v}}$, where $N_a$ is the number of earthquakes in a given time window, $N_e$ is the expected number of earthquakes in a given time window (average event rate times length of window), and $v$ is the variance of earthquakes estimated from the distribution of events in reference time period. Similar to our first analysis, we use an adaptive moving window with a 60 day half-width and a reference period from 12 March 2006 to 1 January 2011. The Beta values will be positive when the seismic rate is higher than the background seismicity rate and negative when it is lower. Additionally, we specifically test for the rate change proposed by *Bouchon et al.* [2016] on 13 January 2011 using the seismicity from 13 January 2011 to 9 March 2011 compared to the year prior to 13 January 2011 for a wide variety of geometry and catalog analysis parameters.

Third, the seismicity is analyzed using a temporal epidemic type aftershock sequence (ETAS) model [*Ogata*, 1992] shown in equation 1.

$$\lambda(t) = \mu(t) + \sum_{t_i<t} \frac{K}{(t - t_i + c)^p} \cdot 10^{\alpha(M_i - M_c)} \quad (1)$$

We compute seismicity rates following *Marsan et al.* [2013] using an iterative smoothing method to select the model parameters describing the target volume. The observed earthquake rate ($\lambda(t)$) is composed of background events ($\mu(t)$) and dependent events, such as foreshocks and aftershocks. In this study we are interested in observing variations of the background rate through time. The second term of equation 1 represents the contribution of aftershocks where $K$ is the aftershock productivity, $\alpha$ is the aftershock efficiency, $c$ and $p$are the Omori decay parameters, and $t_i$ is the time of the $i$th event with a magnitude $M_i$. The best fit inversion parameters are calculated using the entire catalog, and the model parameters are then used to estimate the background seismicity rate curves for the upper and lower planes of seismicity.

During the 2011 Tohoku-oki mainshock there was damage to the Kiban seismic network and in the following months there were many large-magnitude aftershocks. The network conditions and elevated seismicity prohibit the detection of many small events ($M$ < 2) [*Kita*, 2009]; therefore,

we use $M > 2$ events for the ETAS and $\beta$ statistic analysis. For our analysis we assume that changes to the network affect the detection of low-magnitude events in the lower and upper plane equally. Therefore, in order to compare behavior before and after the *M*9.0 rupture, we focus on the ratio of the upper to lower plane seismicity background rates, which we refer to as the intermediate-depth activity ratio. Using the ratio of the seismic activity rates in the upper and lower planes to remove artificial changes in rate resulting from time-dependent detection thresholds was first introduced by *Igarashi et al.*[2002]. Additionally, some large magnitude events (*M*5–6.5) are known to be missing from the hypocenter catalog for a minimum of 25 h following the 2011 Tohoku-oki mainshock due to the large number of recorded events and increased background noise levels [*Kiser and Ishii*, 2013; *Fan and Shearer*, 2016]. While the absence of a few large early aftershocks in the slab would have little effect on rates estimated directly from the catalog, it could bias the ETAS derived background rates. If a large event is missing, the ETAS model rate could be artificially increased by the contamination of aftershocks that were erroneously identified as background events.

## 2.3 Deep Aseismic Slip Rate Estimation From Repeating Earthquakes

In order to explore the interaction between stresses generated by locking of the plate interface and the seismogenesis of intermediate-depth intraplate earthquakes within the slab, we examine temporal variations of deep aseismic fault slip constrained from small repeating earthquakes on the plate interface. Repeating earthquakes are thought to occur on small fault zone asperities with failure being driven by aseismic fault slip on the surrounding fault interface [*Nadeau and Johnson*, 1998; *Uchida and Matsuzawa*, 2013]. In the Tohoku region, repeating earthquakes can provide direct estimates of aseismic fault slip at depth with a spatiotemporal resolution of 20–30 km and 3–12 months, respectively [*Uchida and Matsuzawa*, 2013]. Using a repeating earthquake catalog created by the same procedure as *Uchida and Matsuzawa* [2013], we estimate the cumulative offsets of the small repeating earthquakes downdip of the *M*9.0 Tohoku-oki earthquake. We examine the repeating earthquakes that occur during the 5 years prior to the *M*7.3 foreshock. The same transect geometry previously used to select the JMA hypocenters is used to select the 224 repeating events belonging to 94 sequences shown Figure 1. The aseismic fault slip ($d$) driving each repeating earthquake is estimated using an empirical scaling with seismic moment ($M_0$) [*Nadeau and Johnson,* 1998; *Hanks and Kanamori*, 1979] shown in equation 2.

$$\log(d) = -2.36 + 0.17\ \log(M_0) \quad (2)$$

To study the time-varying aseismic slip downdip of the *M*9.0 Tohoku-oki earthquake, we follow the methods described in *Uchida et al.* [2016] to calculate average slip rates from clusters of

repeater sequences. Rather than using the recurrence interval to obtain a slip rate estimate for each event, we calculate the average cumulative slip rate within a given time period by dividing the total cumulative slip within a given time period by the number of repeater sequences and the duration of the time window. We use the adaptive moving window mentioned previously, with a 90 day half-width and 30 day time steps. Due to detection issues previously mentioned, we do not interpret the deep aseismic slip rates during the 180 days directly following the *M*9.0 mainshock.

# 3 Results

## 3.1 Averaged Seismicity Rates

The 30 day moving-average intermediate-depth earthquake rates from March 2006 through October 2015 for four choices of catalog minimum magnitude thresholds are shown in Figure 2a. We test a range of window sizes from 5 to 100 days and obtain similar results. The rate and cumulative event count curves for minimum magnitudes ranging from *M*1.5 to 3.0 show little to no observable deviation from their average long-term rates prior to the 9 March 2011 *M*7.3 foreshock (Figures 2b and S1), which we refer to throughout as the "preforeshock period." A few short-lived excursions from the long-term average in March 2010, April 2011, November 2012, and November 2013 are coincident with a *M*5.5 event at 78 km depth on 13 March 2010, a *M*7.2 event at 66 km depth on 7 April 2011, a *M*5.6 event at 48 km depth on 25 November 2012, and a *M*7.1 at 56 km depth on 26 November 2013. During the 2 months after the mainshock there is a dramatic drop in the number of small events recorded ($M < 2.0$) that does not recover to constant background levels until May–July 2011 (Figures 2a and S2). For all cutoff magnitudes we find a large sudden increase in the earthquake occurrence rate following the *M*9.0 mainshock, which decays over the following half year to an elevated mean long-term occurrence rate which persists throughout the observation period. The mean rate calculated for events with $M > 2.0$ increased from $0.54 \pm 0.2$ events per day during the preforeshock period to $0.8 \pm 0.3$ since 12 September 2011, the "post 6 month period." The mean rates and variances of the preforeshock and post 6 month periods for all magnitude cutoffs are reported in Table S1.

Figure 2b shows the deep intermediate-depth occurrence rates with the lower and upper planes, respectively. The lower and upper plane shows only minor deviations from the preforeshock average rate prior to the *M*9.0 mainshock. Following the mainshock both planes of seismicity show a sudden increase in occurrence rate. During the post 6 month period the lower plane returns to it preforeshock levels, but with significant variations that are associated with large deep intraplate earthquakes ($M > 6$) located within the lower plane of seismicity. The rate

increase observed at the beginning of 2013 is associated with a *M*7.3 event located at 49 km depth on 7 December 2012; the rate increase observed at the beginning of 2014 is associated with a *M*7.1 event located at 53 km on 26 November 2013. In contrast, the upper plane remains at an elevated occurrence rate throughout the remaining observational period. Figure S3 shows the spatial distribution of the elevated rates observed during the excursion that occurred from March 2007 to July 2008, the time period directly leading up to the *M*9 mainshock, and the elevated rates during the post 6 month period. The ratio of upper plane to lower plane occurrence rates, shows significant variation throughout the observational period (Figure 2b).

## 3.2 $\beta$ Statistic

Figure 2c shows the calculated $\beta$ statistic for the duration of the observational period. We find stable $\beta$ statistic values close to zero for both the upper and lower plane events during the preforeshock period, suggesting there was little variation from the background rate prior to the *M*9.0 Tohoku-oki earthquake. Following the *M*9.0 mainshock, the upper and lower plane seismicity indicate a significant rate change with $\beta$ values above 2 for ~1 year.

Table S2 reports the $\beta$ statistic during the period of the proposed rate increase suggested by *Bouchon et al.* [2016] (13 January 2011 to 9 March 2011). We do not observe a statistically significant deviation in the occurrence rate of intermediate-depth events from the average long-term rate for all magnitude ranges tested. In contrast, we do observe a statistically significant increase in the occurrence rate of shallow events (< 60 km depth) with the largest deviation found using $M \geq 3.0$, ($\beta = 7.60$), which is associated with the slow-slip and foreshock episode described by *Kato et al.* [2012] and *Ito et al.* [2013]. Table S3 shows that the $\beta$ statistic results are not sensitive to our choice of analysis parameters (transect width, minimum magnitude, depth range, and reference period length).

## 3.3 ETAS Model Seismicity Rates

The intermediate-depth ETAS-derived earthquake background rates for both the upper and lower planes of seismicity within the subducting slab are shown in Figure 3a. Following the *M*9.0 mainshock, we observe a large jump in the background rate of events in the upper plane for ~6 months, which then decays to a new background level that is increased to ~150% of the preearthquake long-term rate. In the lower plane of seismicity the rates remain nearly constant and do not significantly deviate from the long-term trend.

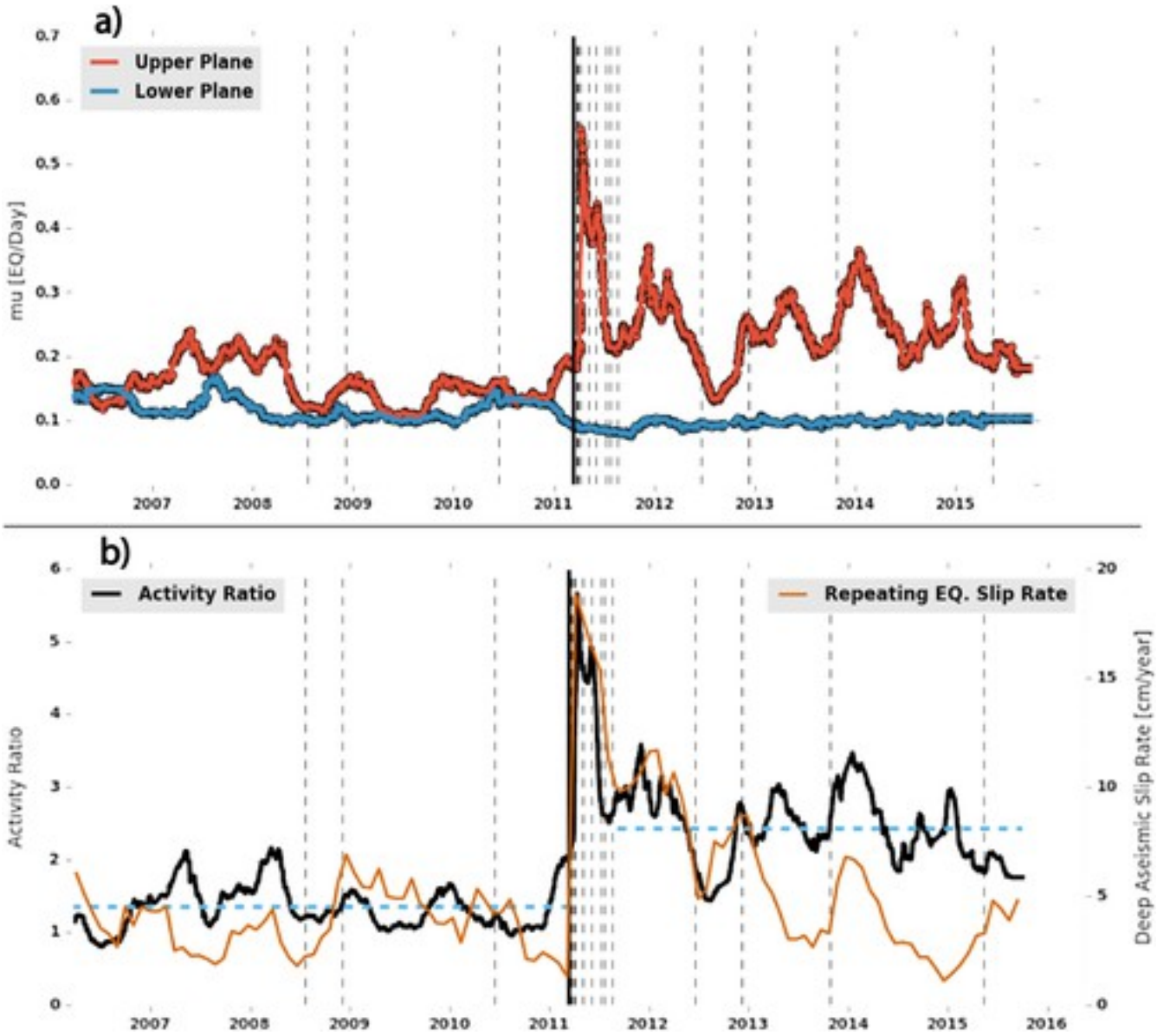


**Figure 3**

**Open in figure viewerPowerPoint**

Intermediate-depth earthquake rates estimated from the ETAS model using $M > 2$ events and deep aseismic slip rates. Curves in both panels represent 30 day moving averages with 12 h steps. (a) The red and blue curves represent background rates for the upper plane and the lower plane, respectively. (b) The ratio of the background rates of the upper and lower planes, termed the activity ratio, is shown by the black line. The deep aseismic slip rate estimated from repeating earthquakes in Figure 1 is shown by the orange line. The dashed horizontal blue lines represent the average value before and after the *M*9.0 Tohoku-oki mainshock, excluding the 6 months following the mainshock. The vertical black dashed lines show the origin times of large magnitude earthquakes ($M > 6.0$) within the transect. The solid black line shows the time of the *M*9.0 March 11 Tohoku-oki mainshock.

Figure 3b shows the intermediate-depth activity ratio. The ratio of background rates for the upper and lower planes is examined to test for a systematic change in earthquake activity from intraslab

stress changes induced by the *M*9.0 mainshock, subsequent large-magnitude aftershocks and postseismic deformation processes. Prior to the mainshock the activity ratio of the upper and lower planes is measured to be 1.4 ± 0.3, implying that the occurrence rate in the upper plane was ~40% greater in the upper plane than in the lower plane (Figure 3b, blue dashed line). At the time of the 2011 Tohoku-oki mainshock, we see a sharp increase in the seismicity rate with the event rate ratio elevated for several months following the mainshock before decreasing to an approximately constant ratio. The activity ratio following the mainshock, excluding the 6 months directly following the mainshock, is 2.5 ± 0.1, implying that the occurrence rate in the upper plane now exceeds the occurrence rate in the lower plane by 150%. The average activity ratio during post 6 month period was found to be 1.8 times greater than the average during the preforeshock period.

### 3.4 Deep Aseismic Slip Rates

The average aseismic slip rate calculated from repeating earthquake sequences downdip of the Tohoku-oki rupture is shown by the orange curve in Figure 3b. During the 5 years prior to the *M*7.3 foreshock, we observe that the deep aseismic megathrust slip rates were relatively low with an average rate of approximately half the plate convergence rate (4.9 cm/yr). Directly following the September 2011 *M*9.0 mainshock, the deep aseismic slip rate increased to a maximum elevated rate of approximately 7 times the plate convergence rate (~60 cm/yr). During the 4 years following the mainshock the aseismic slip rate steadily decayed to a final value of 15.8 cm/yr (September 2015) and an average post 6 month rate of 18.3 cm/yr. The average deep aseismic slip rate during the post 6 month period was found to be 3.7 times greater than the average rate during the preforeshock period. Both before and after the mainshock, quasiperiodic changes in the deep aseismic slip rate roughly correspond to similar variations in the activity ratio. As the rate changes in the repeaters appear to precede those in the activity ratio, this may suggest that variations in the deep aseismic slip can result in observable modulation of deep intraslab seismicity. However, more comprehensive observations and careful modeling are required to test this inference.

## 4 Discussion

### 4.1 Seismicity Prior To the *M*7.3 Foreshock

We have examined the temporal behavior of shallow and intermediate-depth earthquakes near the rupture area of the 2011 *M*9.0 Tohoku-oki earthquake. We do not observe an anomalous precursory increase in intermediate-depth earthquake activity when selecting reasonable choices of geometry, timespan, and minimum magnitude. Prior to the *M*7.3 foreshock we observe

evidence for an increase in the rate of shallow events, which is thought to be associated with slow slip near the hypocenter of the mainshock [*Kato et al.*, 2012]. The earthquake occurrence rate estimates shown in Figure 2a, the individual upper/lower plane occurrence rates shown in Figure 2b, the $\beta$ statistic time series shown in Figure 2c, and the intermediate-depth background rate estimates from the ETAS analysis shown in Figure 3 do not show the precursory activity reported in *Bouchon et al.* [2016].

The results of the statistical tests designed to specifically determine the significance of the precursory activity proposed by *Bouchon et al.* [2016] reported in Table S2 show that there is no evidence for a corresponding change in the rate of intermediate-depth earthquakes. Table S3 shows that this is a robust observation and is not dependent on our choices of geometry or analysis parameters. Figure S2 shows the earthquakes selected from the JMA hypocenter catalog using identical geometries and analysis parameters reported in *Bouchon et al.* [2016]. We are able to reproduce their reported rate increase in intermediate-depth events (depth > 80 km, $M > 1.0$) and shallow events (depths <40 km, $M > 4.0$). However, the increase in intermediate-depth events is only observed for a magnitude cutoff of $M1.0$ (red curve in Figure S3a). The increase in rate above the background rate is not observed for minimum magnitude cutoffs ranging from $M1.5$ to $M3.0$ (Figure S3a). Table S4 reports the $\beta$statistic using the geometry and analysis parameters of *Bouchon et al.* [2016] and qualitatively confirms the observations in Figure S3a ($M \geq 2$, $\beta \approx 0$). Figure S3b shows that there is no deviation from the long-term average background rate for all magnitude ranges considered when the time period used to estimate the background rate is extended to include the 5 years prior to the $M7.3$ foreshock.

The precursory “plunge” mechanism proposed by *Bouchon et al.* [2016] seems to imply an increase in tensile stress prior to the $M9.0$ mainshock resulting from deep slab processes. We argue that an overall increase in intermediate earthquake rates is not expected to be associated with an increase in downdip tensional stress due to the heterogeneity of the background stress field in the subducting slab with the upper plane in downdip compression and the lower plane in downdip extension. Namely, we expect that a downdip tensional stress perturbation would result in an increase in earthquake occurrence rate in the lower plane and suppression of earthquake activity in the upper plane. Our results do not indicate such behavior prior to the $M9.0$ mainshock. Rather, the ETAS derived rates are consistent with increased downdip compression during the time of the proposed rate change of *Bouchon et al.* [2016]. We argue that the precursory activity reported by *Bouchon et al.* [2016] reflects the stress fields associated with long-term mechanical subduction processes late in the earthquake cycle [*Dmowska et*

*al*., 1988; *Uchida et al*., 2013] and previously identified precursory shallow slow slip [*Kato et al*., 2012] rather than short-term precursory extensional accelerations termed “plunges.”

## 4.2 Seismicity Following the *M*9.0 Mainshock

Due to the large rupture area and displacement of the *M*9.0 mainshock, there is a 10–100 kPa increase in downdip compressional stress following the *M*9.0 mainshock in the section of the slab hosting the intermediate-depth earthquakes [*Hu et al*., 2016]. We observe a sharp increase in the ETAS-derived upper plane background rates directly following the *M*9.0 mainshock. In contrast, the ETAS-derived lower plane background rates show little to no deviation from the long-term average. This slight decrease is in contrast with the $\beta$statistic time series results shown in Figure 2c, which suggest that there was a short duration increase in the lower plane occurrence rate following the *M*9.0 mainshock that can also be seen in Figure 2b. This apparent difference between the ETAS- and $\beta$ statistic-derived rate change is likely due to aftershocks from several large events at the base of the upper plane extending into the lower plane, such as the 7 April 2011 *M*7.2 earthquake which occurred at a depth of 66 km. In this case, ETAS background rates will not increase even if aftershock activity increases seismicity rates within the region.

We interpret the increase in the long-term activity ratio after the Tohoku-oki *M*9.0 mainshock as a downdip compressional static stress increase due to the *M*9.0 mainshock and subsequent aftershocks and persistent postseismic processes such as aftershocks, afterslip, viscous relaxation, or fluid flow. The persistent and steady elevated rate of deep aseismic slip estimated from repeating earthquakes suggests that long-term afterslip contributes to the elevated activity ratio (Figure 3b, orange curve).

*Igarashi et al.* [2002] used the activity ratio to study the spatiotemporal changes in the intermediate-depth earthquake activity of NE Japan. They found similar increases in the activity ratio following large plate boundary thrust events. The rupture of the 28 December 1994 *M*7.6 Sanriku-haruka-oki earthquake exhibited a similar temporal response as the *M*9.0 Tohoku-oki earthquake. Directly following the mainshock, both earthquakes produced several yearlong increases in activity ratio. The intermediate-depth earthquake occurrence rates reported in their study also show modulation by afterslip on the plate interface surrounding the mainshock rupture area.

# 5 Conclusions

We have examined the temporal behavior of intermediate-depth earthquakes near the rupture area of the 2011 *M*9.0 Tohoku-oki earthquake. We find that for reasonable choices of geometry,

timespan, and minimum magnitude, we do not observe an anomalous precursory increase in intermediate-depth earthquake activity. We see no evidence for the precursory rate change proposed by *Bouchon et al.* [2016] before the 9 March 2011 *M*7.3 foreshock, but following the *M*9.0 mainshock, we see an increase in the rate of intermediate-depth earthquakes. The rate increase we observe is isolated to the upper plane of the double-layered seismic zone. The increase in the intermediate-depth intraslab earthquake activity ratio following the *M*9.0 mainshock is likely driven by persistent deep aseismic afterslip and other postseismic deformation processes. Further, the activity ratio shows variations throughout the observational period which roughly corresponds to variations in the deep aseismic slip rate revealed by repeating earthquake sequences. In the future, the intermediate-depth intraslab activity ratio should be compared with time-dependent deep aseismic slip estimates from repeating earthquakes such as those from *Uchida et al.* [2016] over a longer time period and larger spatial extent than considered in this study.

## Acknowledgments

This material is based upon work supported by the National Science Foundation Graduate Research Fellowship under grant DGE1106400 for B.G. Delbridge and C.W. Johnson. The earthquake catalog used in this study is produced by the Japan Meteorological Agency, in cooperation with the Ministry of Education, Culture, Sports, Science and Technology (http://www.data.jma.go.jp/svd/eqev/data/bulletin/hypo.html). The catalog is based on seismic data provided by the National Research Institute for Earth Science and Disaster Resilience, the Japan Meteorological Agency, Hokkaido University, Hirosaki University, Tohoku University, the University of Tokyo, Nagoya University, Kyoto University, Kochi University, Kyushu University, Kagoshima University, the National Institute of Advanced Industrial Science and Technology, the Geographical Survey Institute, Tokyo Metropolis, Shizuoka Prefecture, Hot Springs Research Institute of Kanagawa Prefecture, Yokohama City, and Japan Agency for Marine-Earth Science and Technology. We also used waveform data provided by Hokkaido University, Hirosaki University, Tohoku University, and the University of Tokyo (http://wwweic.eri.u-tokyo.ac.jp/harvest/) for the selection of repeating earthquakes.